Spin-to-orbital angular momentum exchange via reflection from a cone

Masud Mansuripur, Armis R. Zakharian, Ewan M. Wright

Masud Mansuripur, Armis R. Zakharian, Ewan M. Wright, "Spin-to-orbital angular momentum exchange via reflection from a cone," Proc. SPIE 8097, Optical Trapping and Optical Micromanipulation VIII, 809716 (9 September 2011); doi: 10.1117/12.899890

SPIE.

Event: SPIE NanoScience + Engineering, 2011, San Diego, California, United States

Spin-to-orbital angular momentum exchange via reflection from a cone

Masud Mansuripur,* Armis R. Zakharian,† and Ewan M. Wright*

*College of Optical Sciences, The University of Arizona, Tucson, Arizona 85721
†Corning Incorporated, Science and Technology Division, Corning, New York 14831

Abstract. In a recent paper we explored the novel reflection properties of several conical optical elements using numerical simulations based on Maxwell's equations. For example, in the case of a hollow metallic cone having an apex angle of 90º, a circularly-polarized incident beam acquires, upon reflection, the opposite spin angular momentum in addition to an orbital angular momentum twice as large as the spin, whereas a 90º cone made of a transparent material in which the incident light suffers two total internal reflections before returning, may be designed to endow the retro-reflected beam with different mixtures of orbital and spin angular momenta. In the present paper we introduce an approximate analysis based on the Jones calculus to elucidate the physics underlying the reflection properties, and we point to the strengths and weaknesses of the approach.

1. Introduction. It is now well established that electromagnetic (EM) waves carry energy, linear momentum, and angular momentum (AM), and it turns out that two apparently different properties of EM waves can give rise to angular momentum: Circular polarization is one source of AM, which is usually referred to as the spin angular momentum (SAM). The other source is associated with spiral phase variations around a given axis, and known as the orbital angular momentum (OAM) [1-6]. The two types of AM are interchangeable, in the sense that a light beam can be made to interact with one or more optical elements in such a way that its SAM and OAM content (each as a fraction of the beam's total AM) will change as a result of interaction with the optical element(s). For example, a circularly-polarized Gaussian beam, which contains SAM only, may be sharply focused through a high-numerical-aperture lens, producing a focused spot that contains both SAM and OAM [7-9]. Alternatively, a circularly-polarized Gaussian beam may be sent through a specially-designed birefringent medium known as a "tuned q-plate," producing, upon transmission, a reversal of the sense of circular polarization in addition to an optical vortex of topological charge $2q$, with q being an arbitrary integer [10]. While some of these processes may involve a net exchange of AM between the light beam and the optical element that is the catalyst for interconversion (e.g., a q-plate with $q \neq 1$), others will preserve the total AM of the light beam while converting a significant fraction of its SAM to OAM, or vice versa. In a recent paper [11] we used full numerical simulations based on Maxwell's equations to show that such interconversions can be performed with relative ease and flexibility with the aid of a metallic cone or a solid dielectric cone. In the present paper we introduce a simplified analysis based on the Jones calculus to elucidate the physics underlying the reflection properties, and we point to the strengths and weaknesses of the approach.

In preparation for the analysis of reflection from a cone, we describe in Sec. 2 the properties of circularly-polarized light reflected from a 90º metallic wedge. In Sec. 3 we show how the reflection of a circularly-polarized Gaussian beam from a hollow metallic cone endows the reflected beam with two units of OAM. The case of solid dielectric cones involving two total internal reflections will be the subject of Sec. 4. We mention in passing that, although conical reflectors have been studied in the past for their applications in atom traps [12, 13] and as end-reflectors in certain types of lasers [14, 15], their ability to convert optical SAM to OAM (or vice versa) does not appear to have been noticed.

2. Reflection from a metallic wedge. The wedge geometry considered is shown in Fig. 1(a), and consists of two perfectly electrically conducting (PEC) plates joined at 90º. In particular, a right-handed circularly-polarized (RCP) Gaussian beam of free-space wavelength 0.5 μm and having a FWHM of 4.0 μm is incident along the negative z-axis, the wedge being aligned along the x-axis. The two successive bounces from the flat facets of the wedge cause the beam to return along the positive z-axis with the same sense of circular polarization as that of the incident beam (see below). The remaining plots in Fig. 1 show numerical results obtained from Maxwell's equations for (b) $|E_y|$, (c) S_z, and (d) the relative phase between the x and y components of the field, all as functions of the transverse coordinates (x, y) following reflection of the incident field from the wedge. Figures 1(b, c) show that the field remains circularly symmetric upon reflection, whereas Fig. 1(d) confirms that the relative phase is 90º so that the reflected field is indeed RCP.

Next we consider a simplified analysis of the wedge based on the Jones calculus. In particular, one finds the following Jones matrix for reflection from the wedge:

Optical Trapping and Optical Micromanipulation VIII, edited by Kishan Dholakia, Gabriel C. Spalding,
Proc. of SPIE Vol. 8097, 809716 · © 2011 SPIE · CCC code: 0277-786X/11/$18 · doi: 10.1117/12.899890

$$M'_{\xi} = \begin{pmatrix} -1 & 0 \\ 0 & \exp(2\mathrm{i}\xi) \end{pmatrix}, \tag{1}$$

where the matrix element -1 arises due to the x-axis reversal upon double reflection, and ξ is the relative phase per reflection between the x and y polarizations at each interface. Here we note that for the wedge in Fig. 1(a) the x-polarized field is tangential to the interface, so it plays the role of an s-polarized incident field, whereas a y-polarized incident field plays the role of a p-polarized beam, and $\xi = 180°$. Thus, for the case of an incident RCP beam with Jones vector $\bar{E}_{\mathrm{i}} = \mathrm{col}(E_x, E_y) = \mathrm{col}(1, \mathrm{i})$, noting that the incident light propagates along the negative z-axis, the reflected Jones vector is $\bar{E}_r = -\mathrm{col}(1, -\mathrm{i})$, which is also RCP assessed with respect to the positive z-axis.

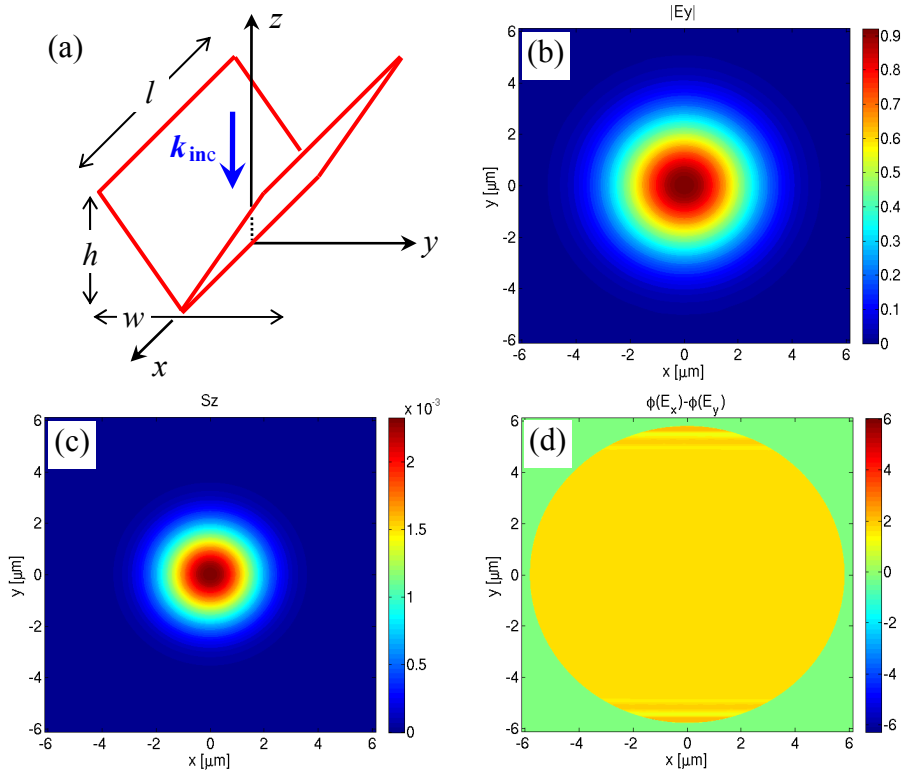

Fig. 1 Maxwell-equations-based simulation of reflection from a wedge-shaped reflector consisting of two PEC sheets joined at 90° along the x-axis. The reflector length, width, and height used in these simulations were $l = w = 12\,\mu\mathrm{m}$, $h = 6\,\mu\mathrm{m}$. The RCP Gaussian beam is incident from above. After two successive reflections at the sheets, the beam returning along the positive z-axis remains right-circularly polarized.

We may take the Jones calculus approach one step further and incorporate the diffraction that must occur as the incident field propagates into and out of the wedge. For this we denote the incident field in Jones vector notation as $\bar{E}_{\mathrm{i}}(x, y) = \mathrm{col}\left[E_x(x, y), E_y(x, y)\right]$, and write the operator for propagation over a distance z as $D(z)$— this operator acts on both vector components of the field. Then we may approximate the reflected field as

$$\bar{E}_r(x, y) = D(h) M'_{\xi} D(h) \bar{E}_{\mathrm{i}}(x, y), \tag{2}$$

where the reflected field $\bar{E}_r(x, y)$ is evaluated at the exit of the wedge of height h. Equation (2) represents a symmetrized split-step approximation to propagation into and out of the cone consisting of free-space propagation into the cone of height h followed by application of the Jones matrix in Eq. (1), and then finally free-space propagation for a distance h out of the cone. Figure 2 shows the simulations based on Eq. (2) corresponding to the Maxwell simulations in

Fig. 1, with excellent overall agreement. In particular, we see that the reflected beam remains circularly symmetric and that the relative phase remains 90º, that is, the reflected beam is RCP.

3. Reflection from a metallic cone. The geometry for the metallic cone is shown in Fig. 3(a), and we shall see below that it shows marked differences in reflection characteristics from the case of the wedge. The Maxwell equation simulation results shown in Fig. 3(b,c,d) reveal that the reflected beam no longer remains Gaussian, but takes on a structure reminiscent of an optical vortex with low intensity at the origin, Figs. 3(b,c), and a 4π phase winding around the cone center; see Fig. 3(d). More specifically, we find that the spin angular momentum associated with the incident RCP beam reverses direction upon reflection, and that the beam also acquires twice as much OAM, associated with its vorticity, in such a way as to precisely cancel out the reversed SAM of the light beam.

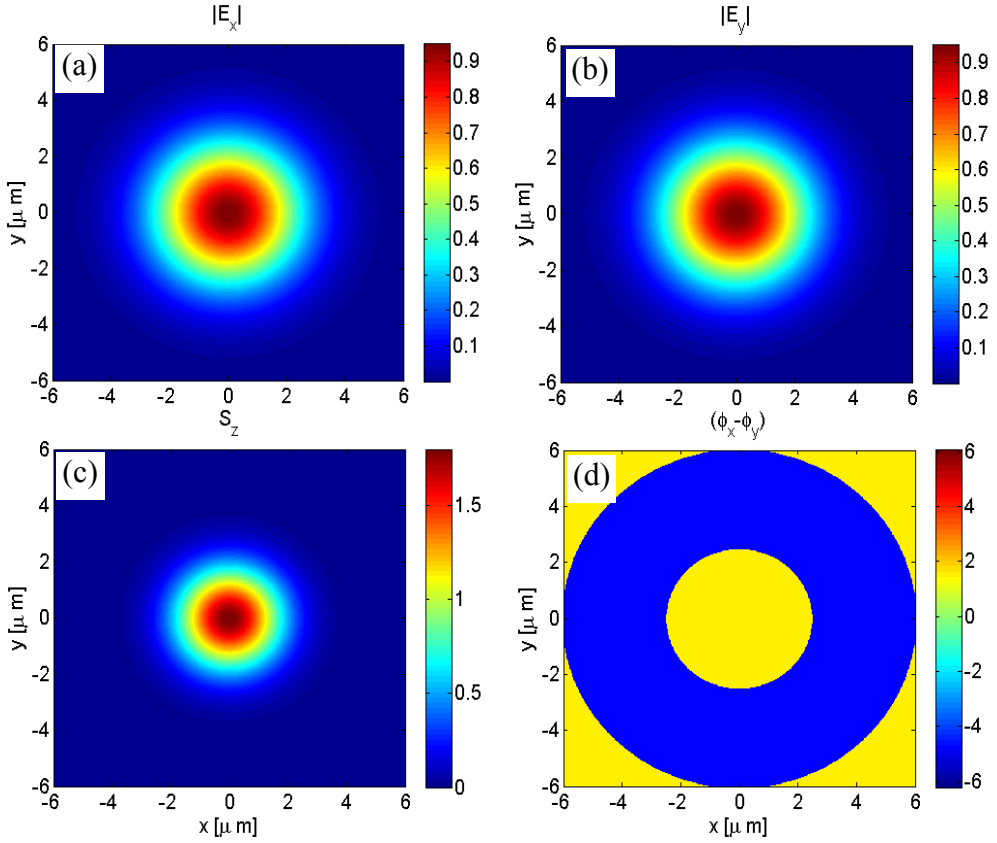

Fig. 2 Simplified Jones calculus simulation of reflection of a Gaussian beam from a wedge-shaped reflector using Eq. (2). The parameters are the same as for Fig. 1.

Figure 3 displays the advertised conversion between SAM and OAM. We may gain insight into the underlying physics by further developing the Jones calculus approach. For this we first note that the Jones matrix must vary with azimuthal angle θ around the cone origin. The reason for this is that the local tangent to the cone, which plays the role of the *s*-polarized direction, and the radial vector direction, which plays the role of the *p*-polarized direction, both rotate with θ. By virtue of this variation, the *s*- and *p*-polarization directions are undefined at the cone origin, meaning that the cone origin presents a singularity. If we choose a basis to coincide with the local *s*- and *p*-polarized directions at the angular position $\theta = 0$ on the cone, the local Jones matrix must be of the form of Eq. (1). For an angular position θ we then have $M_\xi(\theta) = R^{-1}(\theta) M'_\xi R(\theta)$, where $R(\theta)$ is the rotation matrix in two-dimensional space. Evaluating this we find,

$$M_\xi(\theta) = -\exp(i\xi)\begin{pmatrix} \cos(2\theta)\cos(\xi) - i\sin(\xi) & \sin(2\theta)\cos(\xi) \\ \sin(2\theta)\cos(\xi) & -\cos(2\theta)\cos(\xi) - i\sin(\xi) \end{pmatrix}. \quad (3)$$

For the case of the PEC cone in Fig. 3 we set $\xi = 180°$, then for a RCP input $\bar{E}_i = \mathrm{col}(1, i)$ we find $\bar{E}_r = -\exp(2i\theta)\,\mathrm{col}(1, -i)$. The reflected field is therefore RCP with two units of OAM, or winding number 2, around the cone axis in agreement with Fig. 3. The 4π phase spiral associated with the beam reflected from the PEC cone may be interpreted as a Pancharatnam-Berry phase [16,17,18] that arises from the fact that the input beam encircles the singularity at the center of the cone. Incidentally, this terminology is also used in conjunction with the vorticity imparted to a circularly-polarized beam upon passage through a *q*-plate [10].

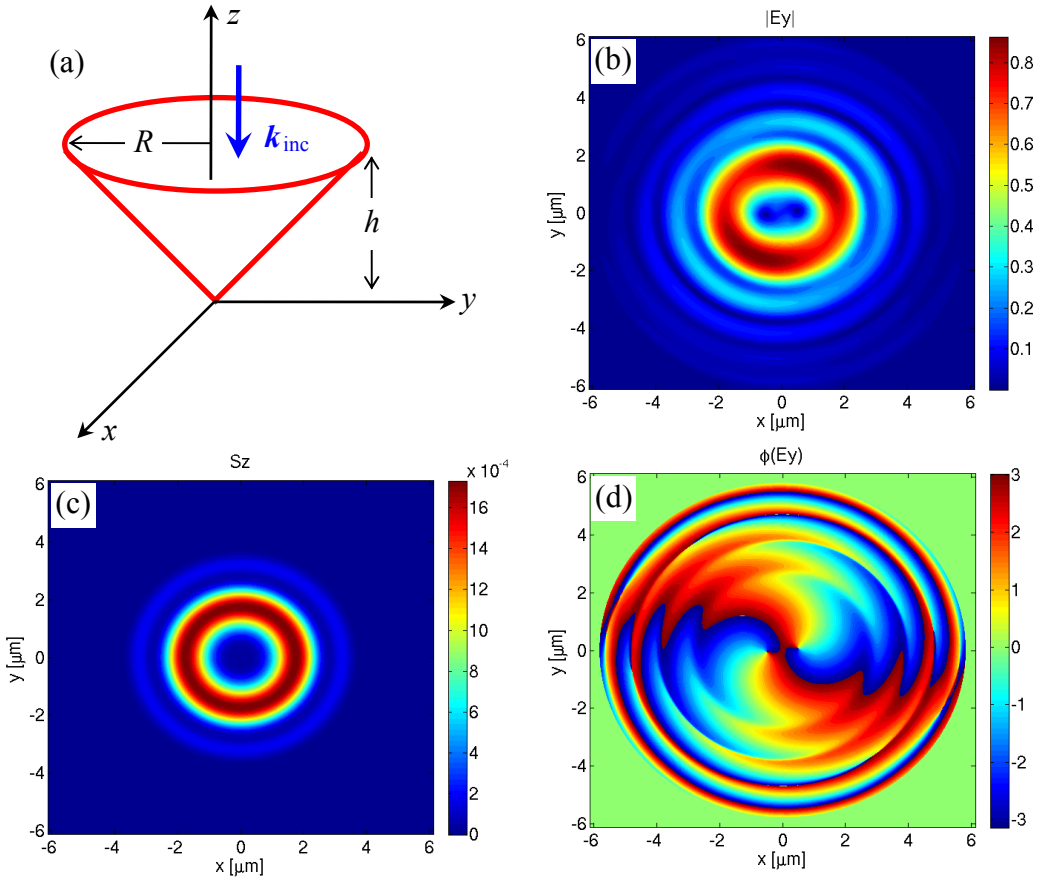

Fig. 3. (a) Hollow PEC conical reflector having a 90º apex angle. In our simulations, the cone's base radius and height were $R = h = 6$ μm. The same RCP Gaussian beam as used in Fig. 1 is incident from above, along the negative *z*-axis. (b) $|E_y|$, (c) S_z, and (d) phase profile of E_y.

We may generalize Eq. (2) for reflection from the PEC cone as follows:

$$\bar{E}_r(x, y) = I_2 D(h) M_\xi(\theta) D(h) \bar{E}_i(x, y), \tag{4}$$

where I_2 performs a two-dimensional inversion around the cone origin. The need for this inversion can be seen by following an input parallel ray and following its path for two reflections through the cone. Figure 4 shows the results from this calculation for the same parameters as in Fig. 3, with very good overall agreement. In particular, we see the 4π phase twist on the reflected beam, Fig. 4(d), and also the doughnut shape of the reflected field, Figs. 4(a,b,c). However, it is clear from the Maxwell-equations-based simulations in Fig. 3 that the 4π phase-winding results from two optical vortices of unity winding number whose cores are slightly off-center, whereas the approximate analysis in Fig. 4 shows a single optical vortex of winding number 2. Furthermore, the approximate analysis yields field profiles that are circularly symmetric, whereas the Maxwell simulations in Fig. 3 show asymmetry in $|E_{x,y}(x,y)|$, although $S_z(x,y)$ remains cylindrically symmetric.

4. Reflection of circularly-polarized light from a transparent dielectric cone. In place of the hollow PEC cone described in Sec. 3, we would now like to employ a solid dielectric cone to retro-reflect the incident Gaussian beam. A first requirement for the dielectric cone is that its refractive index n_{cone} be large enough that the 45º incidence angle on its conical surface exceed the critical angle of total internal reflection (TIR). A second requirement is for the cone to have an anti-reflection coating on its top surface to ensure that the entire beam enters the cone and then, following two internal reflections, leaves the cone. [For numerical computations, the simplest anti-reflection coating is a quarter-wave-thick dielectric layer of refractive index $\sqrt{n_{\text{cone}}}$; see Fig. 5(a).] Even after the above considerations, the dielectric cone differs from the PEC cone in one important respect: the phase difference ξ between the reflected E_p and E_s components of polarization, appearing in the Jones matrix $M_\xi(\theta)$ in Eq.(3), depends on the cone's refractive index, n_{cone}, thus introducing different states of elliptical polarization in the reflected beam.

We present two cases of retro-reflection from conical dielectrics of differing refractive indices in order to understand the various aspects of SAM-to-OAM conversion. Figures 5(b,c,d) show the characteristics of the reflected beam when a 90º glass cone of refractive index $n_{\text{cone}} = 1.55$, base radius = height = 6 μm, coated with a 100 nm-thick layer of refractive index $n_{\text{coat}} = 1.245$, is illuminated with the same RCP Gaussian beam as used in Fig. 1 ($\lambda_o = 0.5$ μm, FWHM = 4 μm). For the chosen n_{cone}, the phase-difference between the *s*- and *p*-components of the light rays after each TIR is $\phi_s - \phi_p = 45º$, resulting in a net phase-shift (upon two reflections) of 90º and, therefore, complete conversion of the incident circular polarization to linear polarization. The reflected beam thus has no SAM, but is endowed with a certain amount of OAM.

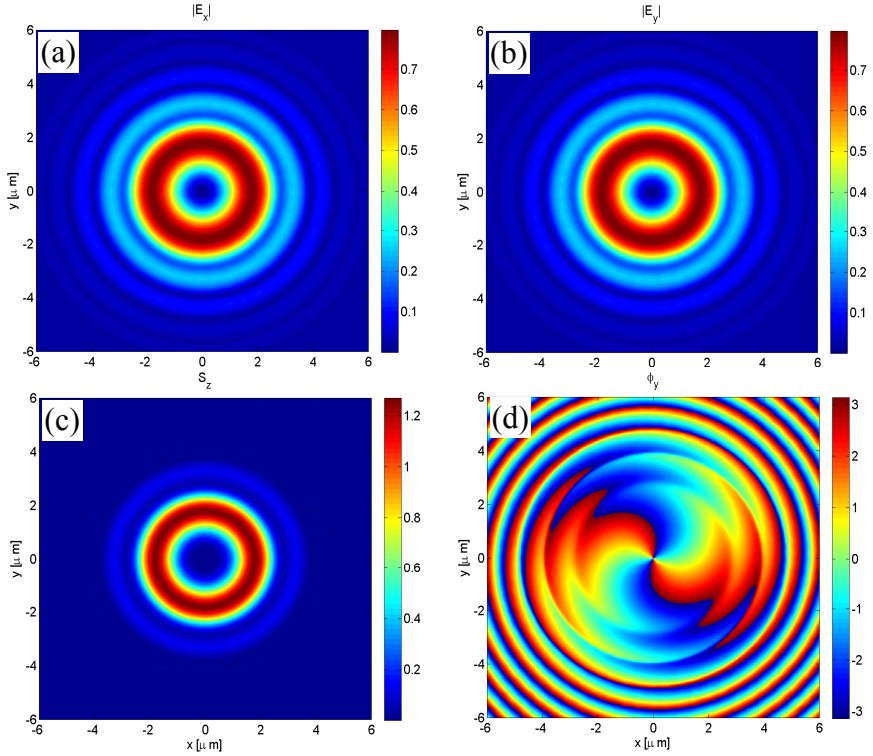

Fig. 4. Jones calculus simulations of reflection from a PEC cone. The same RCP Gaussian beam as used in Fig. 1 is incident on the cone along the negative *z*-axis. (a) $|E_x|$, (b) $|E_y|$, (c) S_z, and (d) phase of E_y.

The reflected beam in this example is linearly polarized, as is revealed in the plot of the relative phase (not shown), which is nearly zero in some regions and almost 180º in others. Both E_x and E_y (Fig. 5(d)) show 4π vorticity in their phase structure, but the corresponding OAM is only half as much as that of a full 4π vortex, because $|E_x|$ and $|E_y|$ (Fig. 5(b)) are not uniformly distributed around *z*. The plot of S_z in Fig. 5(c) is doughnut-like, albeit with a partially-filled hole. The proximity of the 45º angle of incidence on the conical surface to the critical TIR angle of 40.18º is responsible for a small fraction of the incident light leaking out of the cone. In our simulation, the actual fraction of the incident light that returned along +*z* was 92.1%; the corresponding AM of the returning beam was 92.6% that of the incident.

We may use the Jones calculus approach to gain insight into the reflected field using the Jones matrix in Eq. (3) with $\xi = 45°$. In particular, for a RCP input field $\bar{E}_i = \mathrm{col}(1, \mathrm{i})$ the y-component of the reflected field is found to be $E_y = [\mathrm{i}\exp(2\mathrm{i}\theta) - 1]$, that is a superposition of an optical vortex of winding number $\ell = 2$ and a plane-wave. It is well known that such a superposition yields a pair of unit-winding-number optical vortices with separated centers, and this provides an explanation of the vortex splitting evident in Figs. 5(b, d). Further analysis based on the Jones matrix reveals that $|E_x(x,y)|$ should be the same as $|E_y(x,y)|$ in Fig. 5(b) but rotated by 90º, and that the reflected beam should be linearly-polarized as observed in the Maxwell simulations.

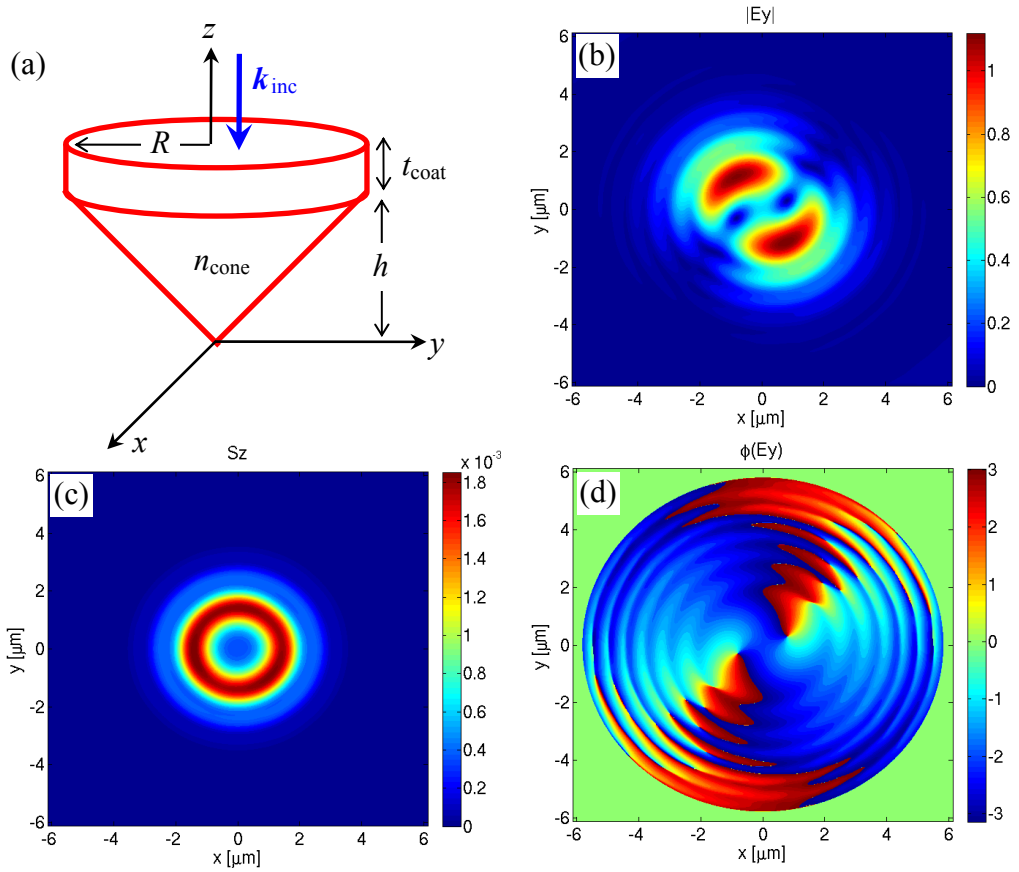

Fig. 5 Maxwell-equations-based simulations of reflection of a RCP Gaussian beam from a glass cone; $n_{cone} = 1.55$, $R = 6$ µm, $h = 6$ µm, $n_{coat} = 1.245$, $t_{coat} = 100$ nm. (a) dielectric cone geometry, (b) $|E_y(x,y)|$, (c) S_z, and (d) phase profile of the y-component of the reflected field.

Figure 6 shows the results for the field reflected from the dielectric cone using the Jones matrix approach and Eqs. (3) and (4) — in the present case, $D(h)$ is the diffraction operator for propagation in the cone medium. While there is good qualitative agreement, we note that the central beam intensity is not as low for the simple model (compare Fig. 5(c) with Fig. 6(c)), but it captures the field magnitude/phase profiles rather well (compare Figs. 5(b,d) with Figs. 6(b,d)).

In our second set of simulations, we chose $n_{cone} = 2.56$, and coated the top facet of the cone with a 78 nm-thick layer of refractive index $n_{coat} = 1.6$. As before, the cone's base radius was equal to its height at 6 µm, and the incident RCP Gaussian beam had $\lambda_o = 0.5$ µm, FWHM = 4 µm. The phase-shift introduced between the s- and p-components after each TIR is now $\phi_s - \phi_p = 79.3°$, resulting in a state of elliptical polarization upon retro-reflection from the cone. Figure 7 shows the characteristics of the reflected beam from the Maxwell simulations in this case. The reflected optical power is now close to 100% of the incident power (i.e., no leakage through the cone). While the incident AM is exclusively due to spin, the reflected beam contains a mixture of SAM and OAM. Figure 8 shows the corresponding simulations based on the Jones calculus with good overall agreement.

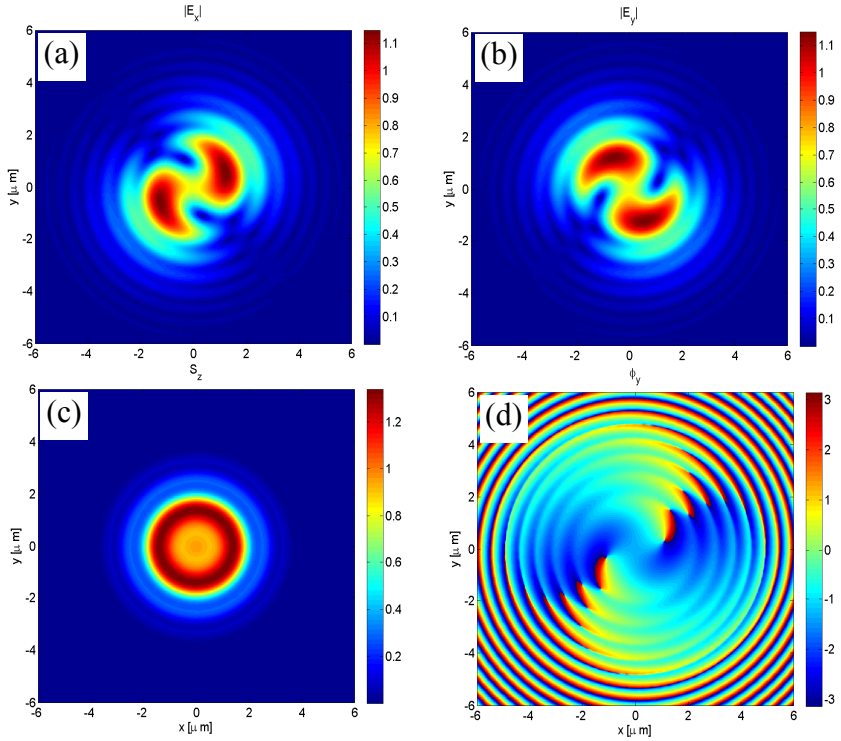

Fig. 6 Jones calculus simulations of reflection of a RCP Gaussian beam from a glass cone ($n_{cone} = 1.55$, $R = h = 6$ μm, $n_{coat} = 1.245$, $t_{coat} = 100$ nm). (a) $|E_x(x,y)|$, (b) $|E_y(x,y)|$, (c) S_z, (d) phase profile of reflected E_y.

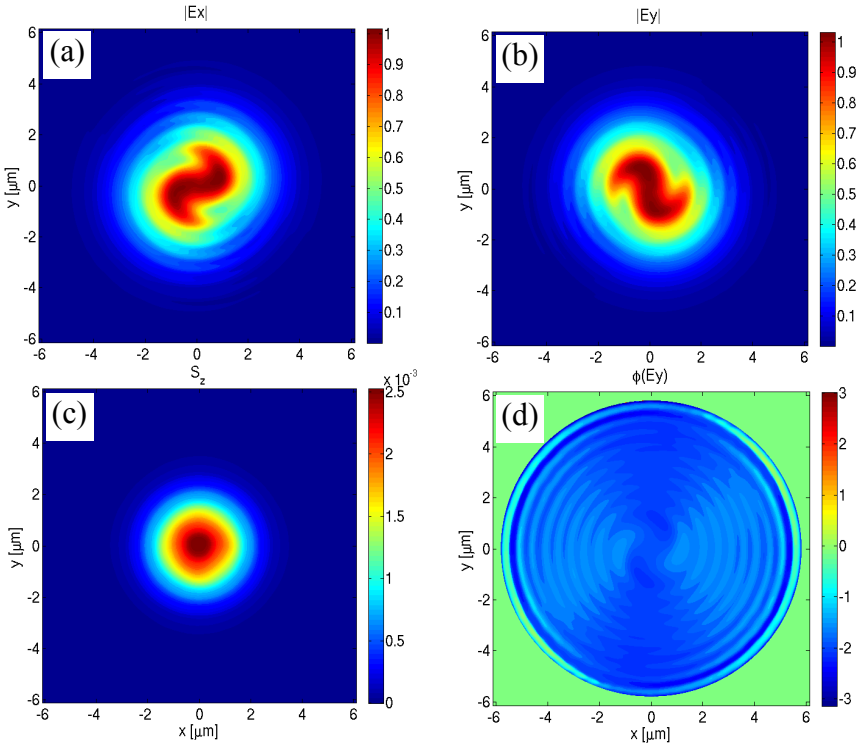

Fig. 7 Maxwell simulation of reflection of a RCP Gaussian beam from a glass cone; $n_{cone} = 2.56$, $R = h = 6$ μm, $n_{coat} = 1.6$, $t_{coat} = 78$ nm. (a) $|E_x(x,y)|$, (b) $|E_y(x,y)|$, (c) S_z, (d) phase profile of reflected E_y.

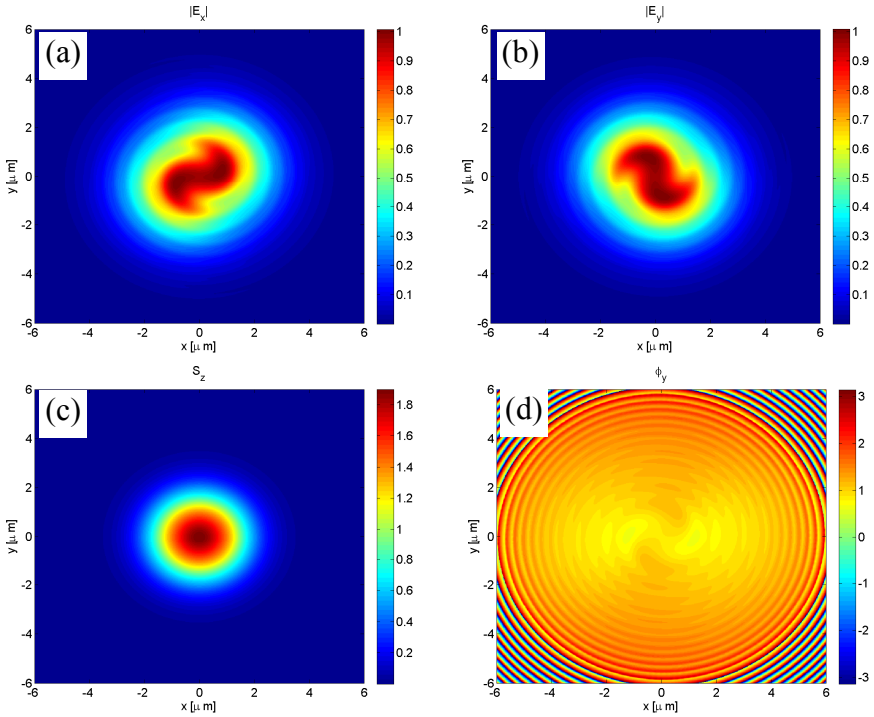

Fig. 8 Jones calculus simulation of reflection of a RCP Gaussian beam from a glass cone; $n_{\text{cone}} = 2.56$, $R = h = 6$ μm, $n_{\text{coat}} = 1.6$, $t_{\text{coat}} = 78$ nm. (a) $|E_x(x,y)|$, (b) $|E_y(x,y)|$, (c) S_z, (d) phase profile of reflected E_y.

5. Concluding remarks. In summary, our goal in this paper was to demonstrate that the physics underlying the spin-to-orbital angular momentum conversion properties of a conical reflector can be elucidated using a simple Jones calculus based approach that also provides good qualitative agreement with simulations based on Maxwell's equations. In contrast to the Maxwell-equations-based simulations that take several hours on a supercomputer, the simulations based on the Jones calculus may be performed in a few seconds on a personal computer. The Jones calculus approach therefore provides a useful qualitative approach to explore light reflection from a PEC cone, and we shall be pursuing this approach in the future.

Acknowledgement. The authors are grateful to Brian Anderson, Poul Jessen, and Timo Nieminen for helpful discussions.

References

1. L. Allen, M. W. Beijersbergen, R. J. C. Spreeuw, and J. P. Woerdman, "Orbital angular-momentum of light and the transformation of Laguerre-Gaussian laser modes," Phys. Rev. A **45**, 8185-8189 (1992).
2. N. B. Simpson, K. Dholakia, L. Allen, and M. J. Padgett, "Mechanical equivalence of spin and orbital angular momentum of light: An optical spanner," Opt. Lett. **22**, 52-54 (1997).
3. L. Allen, M. J. Padgett, and M. Babiker, "The orbital angular momentum of light," Prog. Opt. **39**, 291-372 (1999).
4. J. H. Crichton and P. L. Marston, "The measurable distinction between the spin and orbital angular momenta of electromagnetic radiation," Electronic Journal of Differential Equations, Conference 04 (Mathematical Physics and Quantum Field Theory), pp. 37-50 (2000).
5. A. T. O'Neil, I. MacVicar, L. Allen, and M. J. Padgett, "Intrinsic and Extrinsic Nature of the Orbital Angular Momentum of a Light Beam," Phys. Rev. Lett. **88**, 053601 (2002).
6. S. M. Barnett, "Rotation of electromagnetic fields and the nature of optical angular momentum," J. Mod. Opt. **57**, 1339-1343 (2010).
7. Y. Zhao, J. S. Edgar, G. D. M. Jeffries, D. McGloin, and D. T. Chiu, "Spin-to-Orbital Angular Momentum Conversion in a Strongly Focused Optical Beam," Phys. Rev. Lett. **99**, 073901 (2007).

8. T. A. Nieminen, A. B. Stilgoe, N. R. Heckenberg, and H. Rubinsztein-Dunlop, "Angular momentum of a strongly focused Gaussian beam," J. Opt. A: Pure Appl. Opt. **10**, 115005 (2008).
9. Y. Zhao, D. Shapiro, D. McGloin, D. T. Chiu, and S. Marchesini, "Direct observation of the transfer of orbital angular momentum to metal particles from a focused circularly polarized Gaussian beam," Optics Express **17**, 23316-22 (2009).
10. L. Marrucci, E. Karimi, S. Slussarenko, B. Piccirillo, E. Santamato, E. Nagali, and F. Sciarrino, "Spin-to-orbital conversion of the angular momentum of light and its classical and quantum applications," J. Opt. **13**, 064001 (2011).
11. M. Mansuripur, A. R. Zakharian, and E. M. Wright, "Spin and orbital angular momenta of light reflected from a cone," to be published in Phys. Rev. A (2011).
12. K. I. Lee, J. A. Kim, H. R. Noh, and W. Jhe, "Single-beam atom trap in a pyramidal and conical hollow mirror," Opt. Lett. **21**, 1177-1179 (1996).
13. J. A. Kim, K. I. Lee, H. R. Noh, W. Jhe, and M. Ohtsu, "Atom trap in an axicon mirror," Opt. Lett. **22**, 117-119 (1997).
14. D. Fink, "Polarization effects of axicons," Applied Optics **18**, 581-582 (1979).
15. M. Endo, "Numerical simulation of an optical resonator for generation of a doughnut-like laser beam," Optics Express **12**, 1959-1965 (2004).
16. M. V. Berry, "Quantal phase factors accompanying adiabatic changes," Proc. R. Soc. Lon. A **392**, 45-57 (1984).
17. M. V. Berry, "Interpreting the anholonomy of coiled light," Nature **326**, 277-278 (1987).
18. M. Kitano, T. Yabuzaki, and T. Ogawa, "Comment on 'Observation of Berry's Topological Phase by Use of an Optical Fiber,' " Phys. Rev. Lett. **58**, 523 (1987).